Reaction-Path Dynamics and Theoretical Rate Constants for the $CH_nF_{4-n} + O_3 \rightarrow HOOO + CH_{n-1}F_{4-n}$ ($n = 2,3$) Reactions

Qian Shu Li,*,†,‡ Jing Yang,‡ and Shaowen Zhang‡

School of Chemistry and Environment, South China Normal University, Guangzhou 510006, People's Republic of China, and Institute for Chemical Physics, Beijing Institute of Technology, Beijing 100081, People's Republic of China

Received: April 29, 2006; In Final Form: July 25, 2006

We present a theoretical study of the hydrogen abstraction reactions from CH_3F and CH_2F_2 by an ozone molecule. The geometries and harmonic vibrational frequencies of all stationary points are calculated at the MPW1K, BHandHLYP, and MPWB1K levels of theory. The energies of all of the stationary points were refined by using both higher-level (denoted as HL) energy calculations and QCISD(T)/6-311++G(2df,2pd) calculations based on the optimized geometries at the MPW1K/6-31+G(d,p) level of theory. The minimum energy paths (MEPs) were obtained by the MPW1K/6-31+G(d,p) level of theory. Energetic information of the points along the MEPs is further refined by the HL method. The rate constants were evaluated on the basis of the MEPs from the HL level of theory in the temperature range 200−2500 K by using the conventional transition-state theory (TST), the canonical variational transition-state theory (CVT), the microcanonical variational transition-state theory (μVT), the CVT coupled with the small-curvature tunneling (SCT) correction (CVT/SCT), and the μVT coupled with the Eckart tunneling correction (μVT/Eckart) based on the ab initio calculations. A general agreement was found among the TST, CVT, and μVT theories. The fitted three-parameter Arrhenius expressions of the calculated forward CVT/SCT and μVT/Eckart rate constants of the ozonolysis of fluoromethane are $k^{CVT/SCT}(T) = 2.76 \times 10^{-34}T^{5.81}e^{(-13975/T)}$ and $k^{\mu VT/Eckart}(T) = 1.15 \times 10^{-34}T^{5.97}e^{(-14530.7/T)}$, respectively. The fitted three-parameter Arrhenius expressions of the calculated forward CVT/SCT and μVT/Eckart rate constants of the ozonolysis of difluoromethane are $k^{CVT/SCT}(T) = 2.29 \times 10^{-36}T^{6.42}e^{(-15451.6/T)}$ and $k^{\mu VT/Eckart}(T) = 1.31 \times 10^{-36}T^{6.45}e^{(-15465.8/T)}$, respectively.

1. Introduction

It has long been recognized that the stratospheric ozone layer is of vital importance to life on Earth. It is now widely accepted that chlorofluorocarbons (CFCs) contribute to the "greenhouse effect" and also are responsible for the depletion of the stratospheric ozone layer.[1−7] Thus, a very important international effort has been undertaken to find environmentally acceptable alternatives to CFCs, especially since the production of CFCs was restricted under the Montreal protocol[8] on substances that destroy stratospheric ozone. With low global environmental impact, fluoromethane compounds have been proposed as a potential replacement of the chlorofluorocarbons (CFCs) and greenhouse gases;[3,6,7,9] therefore, it is important to have good estimates of their atmospheric lifetimes to really assess their environmental impact. In this context, kinetic studies of relevant gas-phase reactions involving CH_3F (HFC-41) and CH_2F_2 (HFC-32) would assist in understanding their fates in the atmosphere. A continuous search is underway to try to improve the experimental techniques and the theoretical methodologies that deal with the kinetics of those reactions involving HFCs and HCFCs.

CH_3F (HFC-41) and CH_2F_2 (HFC-32) are very important species in atmospheric study. Although there are some studies about the reactions of fluoromethanes with different species, with $H^{\bullet}$,[10] $CH^{\bullet}$,[11] $Cl^{\bullet}$,[12−14] O^-,[15,16] O_2^-,[15] $OH^{\bullet}$,[17−21] OH^-,[22−24] $F^{\bullet}$,[25] and F^-,[26,27] no data were reported about the direct hydrogen abstraction reaction of ozone with fluoromethanes (CH_3F, CH_2F_2). The reactions of CH_3F (HFC-41) and CH_2F_2 (HFC-32) with ozone are of special significance to atmospheric chemistry. The relevant kinetic data are desirable not only to understand the reaction mechanism but also to determine if the HFCs are really safe for the ozone layer under different conditions. Ozonolysis of CH_3F and CH_2F_2 is the simplest reaction of a reaction class of ozone molecule with fluoromethanes that produce the F-atom substituent alkyl and HOOO oxygen-rich radical. The hydrogen abstraction reactions by ozone from fluoromethanes (CH_3F, CH_2F_2) are the most suitable processes for modeling and testing methodologies that could be applied to larger molecules or to the complete reaction kinetic schemes for the degradation of HFCs. The knowledge of rate constants of these reactions is also of special interest to us because they can produce the important HOOO radical,[28,29] which can dissociate the OH radical and O_2 molecule with a very low barrier. However, to the best of our knowledge, no kinetics data and reaction mechanism of the title reactions were reported. To acquire accurate rate constants over a wide temperature range, both high-level ab initio and rate constant calculations are required.

The objective of this study is to accurately calculate the rate constants of the reactions $CH_nF_{4-n} + O_3 \rightarrow HOOO + CH_{n-1}F_{4-n}$

* Corresponding author. Fax: +86-10-68912665. E-mail: qsli@bit.edu.cn.
† South China Normal University.
‡ Beijing Institute of Technology.

10.1021/jp0626317 CCC: $33.50
Published on Web 09/02/2006

(n = 2,3). For comparison, three levels of hybrid density functional theory methods were employed to investigate the reactions of fluoromethanes (CH_3F, CH_2F_2) with ozone. The thermal rate constants were calculated using the conventional transition-state theory (TST),[30] the canonical variational transition-state theory (CVT),[30−33] the microcanonical variational transition-state theory (μVT),[30,34,35] the CVT coupled with the small-curvature tunneling (SCT) correction (CVT/SCT),[36−38] and the μVT coupled with the Eckart tunneling correction (μVT/Eckart)[39−41] based on the ab initio calculations.

2. Calculation Methodology

2.1. Electronic Structure Calculations. It has been shown that the modified Perdew−Wang one-parameter model for kinetics (MPW1K) method provides a good alternative for a wide variety of applications, in particular, for kinetic studies.[42,43] In the present study, the geometries and frequencies of all stationary points (reactants, products, and the transition states) are optimized at the MPW1K level of theory with the 6-31+G(d,p) basis set. Synchronously, to validate the reliability of the MPW1K method, the same calculations are performed by the BHandHLYP[44,45] and MPWB1K[46−48] levels of theory with the same basis set. We find that the calculated results predicted at these levels of theory are in good agreement with one another. We have also optimized the geometries of the reactants, products, and transition states at the MPW1K/6-311+G(2df,2pd) level of theory to show the impact of basis set effect on structures. The calculated results of MPW1K/6-311+G(2df,2pd) and MPW1K/6-31+G(d,p) agree with each other fairly well in our study. However, it has been recommended that the 6-31+G(d,p) basis set be used for MPW1K by Truhlar.[42] Therefore, the MPW1K/6-31+G(d,p) geometries become our choice as the base of single-point calculations. To yield more reliable reaction enthalpies and barrier heights, single-point calculations for all stationary points are further refined by means of higher-level energy calculations (denoted as HL)[49] based on the optimized geometries at the MPW1K/6-31+G(d,p) level of theory. The HL method employs a combination of QCISD(T)[50] and MP2(FC)[51] methods and can be expressed as:

$$\begin{aligned} E_{\mathrm{HL}} = {} & E[\mathrm{QCISD(T)/cc\text{-}pVTZ}] + \\ & (E[\mathrm{QCISD(T)/cc\text{-}pVTZ}] - \\ & E[\mathrm{QCISD(T)/cc\text{-}pVDZ}])*0.46286 + \\ & E[\mathrm{MP2(FC)/cc\text{-}pVQZ}] + (E[\mathrm{MP2(FC)/cc\text{-}pVQZ}] - \\ & E[\mathrm{MP2(FC)/cc\text{-}pVTZ}])*0.69377 - \\ & E[\mathrm{MP2(FC)/cc\text{-}pVTZ}] - (E[\mathrm{MP2(FC)/cc\text{-}pVTZ}] - \\ & E[\mathrm{MP2(FC)/cc\text{-}pVDZ}])*0.46286 \end{aligned}$$

Here QCISD(T)/cc-pVTZ is referred to as the quadratic configuration interaction calculation including single and double substitutions with a triples contribution to the energy added, using Dunning's[52,53] correlation consistent polarized valence triple-ζ basis set. The cc-pVDZ and cc-pVQZ stand for Dunning's correlation consistent polarized valence double-ξ basis set and polarized valence quadruple-ξ basis set, respectively. MP2(FC) denotes the second-order Moller−Plesset perturbation theory with frozen core approximation.[51] To validate the reliability of the HL method, the single-point calculation of stationary points was also performed at the QCISD(T)/6-311++G(2df,2pd) level of theory. The single-point calculated results predicted at two levels of theory are in good agreement with each other. The HL method includes the extrapolation to the infinite basis set limit and is a dual-level theory, so it may be suggested that the energetic information obtained at the HL level of theory is relatively reliable.[49,54−56] The theoretical standard enthalpy of formation values (obtained by HL method) of CH_3F and CH_2F_2 are 245.43 and 450.48 kJ/mol, respectively. The experimental standard enthalpy of formation values of CH_3F and CH_2F_2 are 247.00 and 450.66 kJ/mol, respectively.[57,58] The little difference between the theoretical and experimental standard enthalpy of formation of reactants suggests that HL is good for estimating the energies of current work. Considering efficiency and veracity synthetically, the minimum energy paths (MEPs) from $s = -1.50$ to 1.50 amu$^{1/2}$ bohr were done in the mass-weighted Cartesian coordinate with a step size of 0.01 amu$^{1/2}$ bohr, using the intrinsic reaction coordinate (IRC) method at the MPW1K/6-31+G(d,p) level of theory. Along this energy path, the reaction coordinate s is defined as the signed distance from the saddle point, with $s > 0$ referring to the product side. At 20 selected points (10 points in the reactant side before the transition state and 10 points in the product side after the transition state selected by focusing technique[39]) along the MEP, the force constant matrixes as well as the harmonic vibrational frequencies were calculated at the same level. Furthermore, the energies of the selected points were refined by the HL method to construct a more accurate potential energy profile. The single-point HL and QCISD(T)/6-311++G(2df,2pd) calculations are based on the optimized geometries at the MPW1K/6-31+G(d,p) level of theory, denoted as HL//MPW1K and QCISD(T)//MPW1K, respectively. All of the above calculations were performed using the Gaussian 03[59] and MOLPRO 2002.6[60] program suites.

2.2. Rate Constant Calculations. The conventional transition-state theory, the canonical variational transition-state theory, and the microcanonical variational transition-state theory were employed to calculate the rate constants for the two bimolecular reactions. There is considerable literature on the TST, CVT, and μVT formalisms. Below, we give only a brief description of them, which has been implemented in the POLYRATE 8.2[61] and Vklab 1.0[62] programs.

Within the transition-state theory (TST)[30] framework, thermal rate constants of a reaction can be expressed as:

$$k(T) = \kappa(T)\sigma\frac{k_{\mathrm{B}}T}{h}\frac{Q^{\ddagger}(T)}{\Phi^{\mathrm{R}}(T)}e^{\{-\Delta V^{\ddagger}/k_{\mathrm{B}}T\}}$$

where κ is the transmission coefficient accounting for the quantum mechanical tunneling effects, σ is the reaction symmetry number, $Q^{\ddagger}$ and Φ^{R} are the total partition functions (per unit volume) of the transition state and reactants, respectively, $\Delta V^{\ddagger}$ is the classical barrier height, T is the temperature, and k_{B} and h are the Boltzmann and Planck constants, respectively.

The variational transition-state rate constant for a gas-phase bimolecular reaction is determined by varying the location of the dividing surface along a reference path to minimize the rate constant at a given temperature. In other words, CVT minimizes the recrossing effects by effectively moving the dividing surface along the minimum energy path (MEP) so as to minimize the rate constant. In the present study, the MEP is defined as the steepest descent path from the saddle point to both the reactant and the product sides in the mass-weighted Cartesian coordinate system. The reaction coordinate, s, is defined as the distance along the MEP with the origin located at the saddle point and is positive on the product side and negative on the reactant side. For a canonical ensemble at a given temperature T, the canonical variational transition-state theory (CVT)[31−33] thermal rate

constant $k^{CVT}(T)$ is given by

$$k^{CVT}(T) = \min_s k^{GT}(T,s)$$

where

$$k^{GT}(T,s) = \left\{ \sigma \frac{k_B T}{h} \frac{Q^{GT}(T,s)}{\Phi^R(T)} e^{-V_{MEP}(s)/k_B T} \right\}$$

where $k^{GT}(T,s)$ is the generalized transition-state theory rate constant at the dividing surface that intersects the MEP at s and is orthogonal to the MEP. Here, σ is the symmetry factor accounting for the possibility of more than one symmetry-related reaction path, k_B is Boltzman's constant, and h is Planck's constant. Q^{GT} is the internal partition function of the generalized transition state with the local zero of energy at $V_{MEP}(s)$. Φ^R is the reactant partition function (per unit volume for bimolecular). Translational and rotational partition functions were evaluated classically, whereas the vibrational partition functions were calculated quantum mechanically within the harmonic approximation in the present studies.

The microcanonical variational transition-state theory (μVT)[30,34,35] is based on the idea that by minimizing the microcanonical rate constants along the MEP, one can minimize the error caused by the "recrossing" trajectories. Within the framework of μVT, the rate constant at a fixed temperature T can be expressed as:

$$k^{\mu VT}(T) = \frac{\int_0^\infty \min\{N^{GTS}(E,s)\} e^{-E/k_B T} dE}{h\Phi^R}$$

where Φ^R is the total reactant partition function, which is the product of electronic, rotational, and vibrational partition functions. The relative translational partition function was calculated classically and is included in Φ^R. However, the rotational and vibrational partition functions of the reactant were calculated quantum mechanically within the rigid rotor and harmonic oscillator approximations, respectively. $N^{GTS}(E,s)$ is the sum of states of electronic, rotational, and vibrational motions at energy E of the generalized transition state located at s, where s is the reaction coordinate.

In addition, both of the two reactions involve hydrogen-transfer processes. For such steps, tunneling is expected to be noticeable. The SCT tunneling method[36−38] was employed to calculate the transmission coefficient in the calculation of the CVT rate constant, and the Eckart tunneling method[39,40] was employed to calculate the transmission coefficient in the calculation of the μVT rate constant.

3. Results and Discussion

3.1. Stationary Points. The optimized geometric parameters of all of the reactants, products, and transition states at the MPW1K/6-31+G(d,p), BHandHLYP/6-31+G(d,p), and MPWB1K/6-31+G(d,p) levels of theory along with the MPW1K/6-311+G(2df,2pd) level of theory are given in Figure 1. The geometries of the main stationary points are also shown in Figure 1. The TS(1) is the transition state of the reaction of ozone with fluoromethane, and the TS(2) is the transition state of the reaction of ozone with difluoromethane. From the results listed in Figure 1, it can easily be seen that the optimized geometries for CH_3F and CH_2F_2 are C_{3V} and C_{2V} symmetries, respectively. The bond lengths and bond angles for the reactants and the products obtained from different computational techniques are

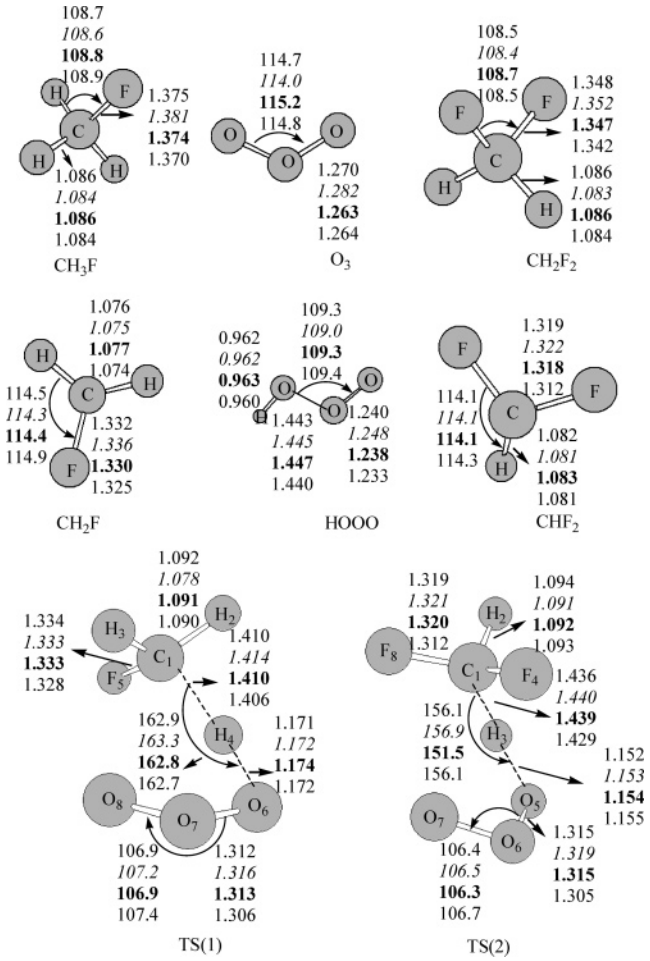

Figure 1. Optimized geometries of the reactants, products, and transition states of studied reactions. Parameters are given in the order (top to bottom): MPW1K/6-31+G(d,p) in normal print, BHandHLYP/6-31+G(d,p) in italics, MPWB1K/6-31+G(d,p) in bold, and MPW1K/6-311+G(2df,2pd) in normal print. Bond lengths are in angstroms, and angles are in degrees.

in good agreement with one another. Furthermore, the calculated structural parameters for all of the stationary points at the MPW1K/6-31+G(d,p) level of theory are slightly closer to those calculated at the levels of MPW1K/6-311+G(2df,2pd) and MPWB1K/6-31+G(d,p) than the results obtained from the BHandHLYP method. For the transition-state structure in each reaction, the lengths of the breaking C−H bond in TS(1), TS(2), increase by 29.8% and 32.1%, respectively, with respect to the corresponding equilibrium bond lengths of the reactants CH_3F and CH_2F_2 at the MPW1K/6-31+G(d,p) level of theory. Meanwhile, the lengths of the forming O−H bond in each transition state, which will form a HOOO radical, are 21.7% and 19.8% longer, respectively, than the equilibrium bond lengths of the HOOO radical. Therefore, the geometry features of TS(1) and TS(2) are similar to the structure parameters for ozone and the fluoromethanes, and this is characteristic for early transition states.

Table 1 lists the harmonic vibrational frequencies and zero-point energies of reactants, products, and transition states at the MPW1K/6-31+G(d,p) level of theory along with the available experimental data. From Table 1, one can find that the calculated frequencies at the MPW1K/6-31+G(d,p) level of theory are consistently larger than the corresponding experimental values.[63−67] However, the discrepancy between theoretical results and experimental data is generally within 9%. This shows that the calculated frequencies are in good agreement with the

TABLE 1: Harmonic Vibrational Frequencies (cm^{-1}) and Zero-Point Energy (kcal mol^{-1}) of the Reactants, Products, and Transition States Using the MPW1K Method with the Basis Set 6-31+G(d,p)

species	frequencies	ZPE
CH_3F	1124, 1228, 1228, 1528, 1537, 1537, 3133, 3234, 3234	25.4
expt[a]	1154, 1185, 1397, 3078	
CH_2F_2	541, 1169, 1176, 1214, 1314, 1504, 1578, 3071, 3253	21.3
expt[a]	528, 1090, 1111, 1178, 1262, 1435, 1508, 3014	
CH_2F	590, 1205, 1237, 1511, 3242, 3404	16.0
expt[a]	1170, 1515	
CHF_2	561, 1039, 1233, 1254, 1392, 3245	12.5
expt[a]	1164, 1173, 1317	
O_3	790, 1159, 1228	5.2
expt[a]	716, 1089, 1135	
HOOO	61, 571, 843, 1328, 1478, 3920	11.7
TS(1)	1501i, 91,[b] 163, 285, 432, 583, 766, 878, 1110, 1185, 1220, 1238, 1290, 1308, 1523, 1840, 3129, 3319	29.1
TS(2)	1470i, 87,[b] 153, 206, 388, 525, 535, 597, 830, 1133, 1179, 1212, 1243, 1280, 1321, 1427, 1928, 3120	24.5

[a] References 63−67. [b] i denotes the imaginary frequency.

TABLE 2: Reaction Energetics Parameters (kcal mol^{-1}) at the HL//MPW1K/6-31+G(d,p) and QCISD(T)//MPW1K/6-31+G(d,p) Levels of Theory

method	ΔE^a	$\Delta H_{298K}°$	$V^{\ddagger\,b}$	$V_a^{G\ddagger\,c}$
$CH_3F + O_3 \rightarrow CH_2F + HOOO$				
HL//MPW1K	23.10	23.77	37.13	36.64
QCISD(T)//MPW1K	23.08	23.75	36.52	36.03
$CH_2F_2 + O_3 \rightarrow CHF_2 + HOOO$				
HL//MPW1K	23.31	23.88	40.15	38.96
QCISD(T)//MPW1K	22.46	23.03	39.22	38.03

[a] Reaction energy with zero-point energy correction. [b] The classical potential barriers. [c] The adiabatic barriers at the saddle point structure.

available experimental values. For the transition state, the character of the stationary points is confirmed by normal-mode analysis, which yield only one imaginary frequency whose eigenvector corresponds to the direction of the reaction. The absolute values of imaginary frequencies at the MPW1K/6-31+G(d,p) level of theory for TS(1) and TS(2) are 1501 and 1470 cm^{-1}, respectively. It can also be seen that the transition state possesses a large absolute value of the imaginary frequency. This indicates that the quantum tunneling transmission coefficient should be larger and the quantum tunneling effects should be important in the calculations of the rate constants.

The reaction energies (ΔV), the classical potential barriers ($V^{\ddagger}$), the vibrationally adiabatic ground-state potential ($V_a^{G\ddagger}$), and the reaction enthalpies ($\Delta H_{298K}°$) calculated at the HL//MPW1K and QCISD(T)//MPW1K levels of theory are listed in Table 2. Note that the values of $V^{\ddagger}$ and $V_a^{G\ddagger}$ are calculated at the corresponding saddle points. The predicted values of these properties are quite scattered between the two different methods. For the reactions of ozone with fluoromethane and ozone with difluoromethane, the refined reaction enthalpies are 23.77 and 23.88 kcal mol^{-1} at the HL level of theory based on the geometries optimized at the MPW1K/6-31+G(d,p) level of theory, respectively. The predicted reaction enthalpies from the QCISD(T)//MPW1K levels of theory are slightly smaller than those from the HL method. The same trend also appears for the vibrationally adiabatic ground-state potentials. This means that the MPW1K/6-31+G(d,p) level of theory can provide reasonable geometric information[42] but additional single-point HL calculations are needed to get accurate energetic information. As can be seen from Table 2, it is obvious that the forward barrier heights of the ozonolysis of fluoromethane are smaller than those of ozonolysis of difluoromethane. Consequently, it could be anticipated that the rate constant of the reaction of ozone with fluoromethane will be larger than that of ozone with difluoromethane. With the increase of the number of fluorine substitutions, the forward barrier heights increase. This reflects that the fluorine substitution can affect the H-abstraction process.

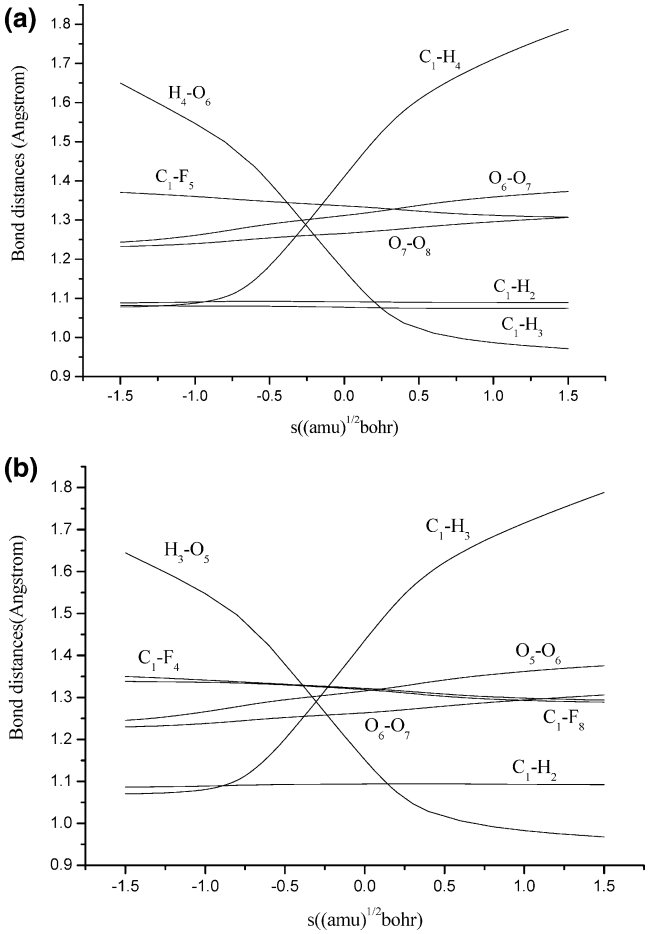

Figure 2. Bond distance curves of the reactions as a function of reaction coordinate s ((amu)$^{1/2}$ bohr) at the MPW1K/6-31+G(d,p) level of theory: (a) The reaction of ozone with fluoromethane. (b) The reaction of ozone with difluoromethane. The numberings of the atoms can be seen from Figure 1.

3.2. Reaction Path Properties. As a reasonable compromise between speed and accuracy, the geometries of points along the MEP were optimized at the MPW1K/6-31+G(d,p) level of theory. Starting from the MPW1K saddle-point geometries, and going downhill to both the asymptotic reactant and the product channels in mass-weighted internal coordinates (with no reorientation and no use of symmetry), we constructed the intrinsic reaction path (IRC). The potential energy profiles were then further refined at the HL//MPW1K level of theory.

Figure 2 shows the variation of the bond lengths along the minimum energy path of the bimolecular reactions as a function of reaction coordinate s ((amu)$^{1/2}$ bohr) at the MPW1K/6-31+G(d,p) level of theory. For the reaction of ozone with fluoromethane, it is seen from Figure 2a that the change of the C1−H4 bond length remains insensitive up to $s = -0.8$ amu$^{1/2}$ bohr and then increases smoothly afterward with the increase of the IRC coordinate. However, the H4−O6 bond length decreases smoothly to the H−O bond distance of HOOO radical. This means that the process of forming the H4−O6 bond and breaking the C1−H4 bond of the H-abstraction reaction takes place synergistically along the MEP. The variation of the O6−O7 and O7−O8 bond distances is mild along the whole MEP

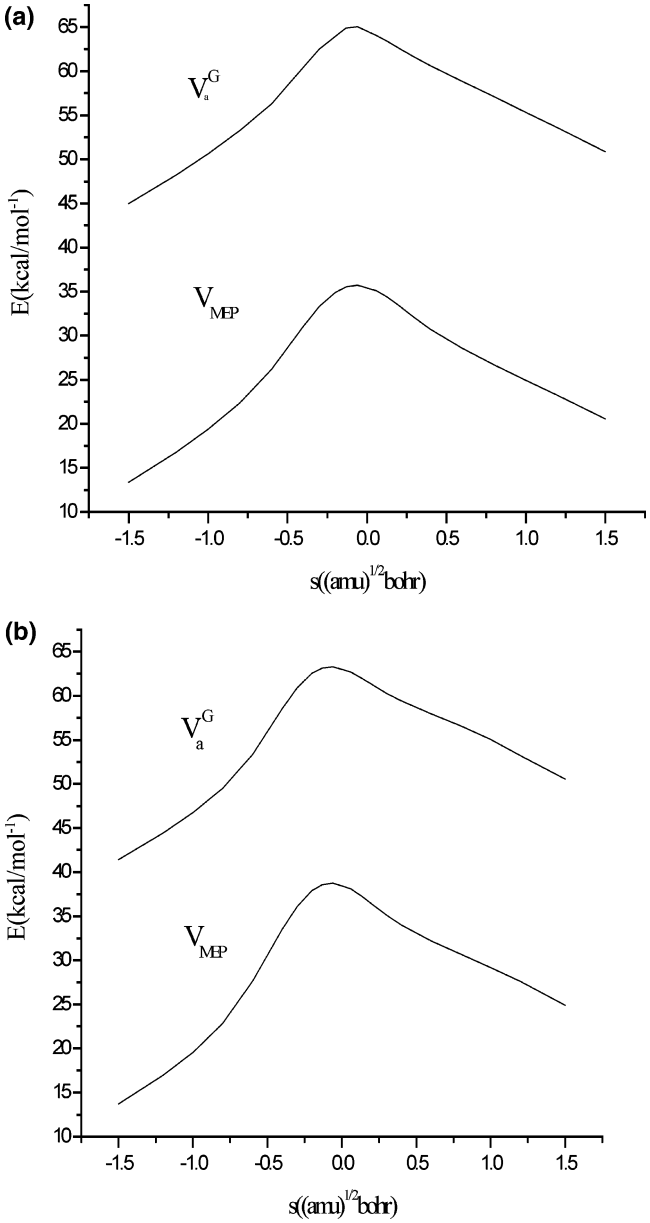

Figure 3. Classical potential energy (V_{MEP}) and the ground-state vibrationally adiabatic potential energy (V_a^G) curves of the reactions as functions of the reaction coordinate *s* at the HL//MPW1K/6-31+G(d,p) level of theory: (a) The reaction of ozone with fluoromethane. (b) The reaction of ozone with difluoromethane.

as compared to the C1−H4 bond of the H-abstraction process, and the C1−H2 and C1−H3 bond lengths are almost unchanged during the reaction process. For the reaction of ozone with difluoromethane (Figure 2b), the breaking C1−H3 bond length almost linearly increases, while the forming H3−O5 bond length of the HOOO radical gradually shortens in the course of the reaction. This means that the synergetic process of forming the H3−O5 bond and breaking the C1−H3 bond of the H-abstraction reaction takes place.

The classical potential energy curves (V_{MEP}) and vibrationally adiabatic ground-state potential energy curves (V_a^G) of both channels as functions of the reaction coordinate *s* ((amu)$^{1/2}$ bohr) are presented in Figure 3 at the HL level of theory. As can be seen, the positions of the maximum of the $V_{MEP}(s)$ and the $V_a^G(s)$ energy curves are the same, and the two curves are very similar in shape for each reaction. Around the top of V_{MEP} and V_a^G, the curves of the ozonolysis of fluoromethane are slightly flatter than those of ozonolysis of difluoromethane, which may result in a stronger quantum transmission effect of the ozonolysis of difluoromethane than that of the ozonolysis of fluoromethane.

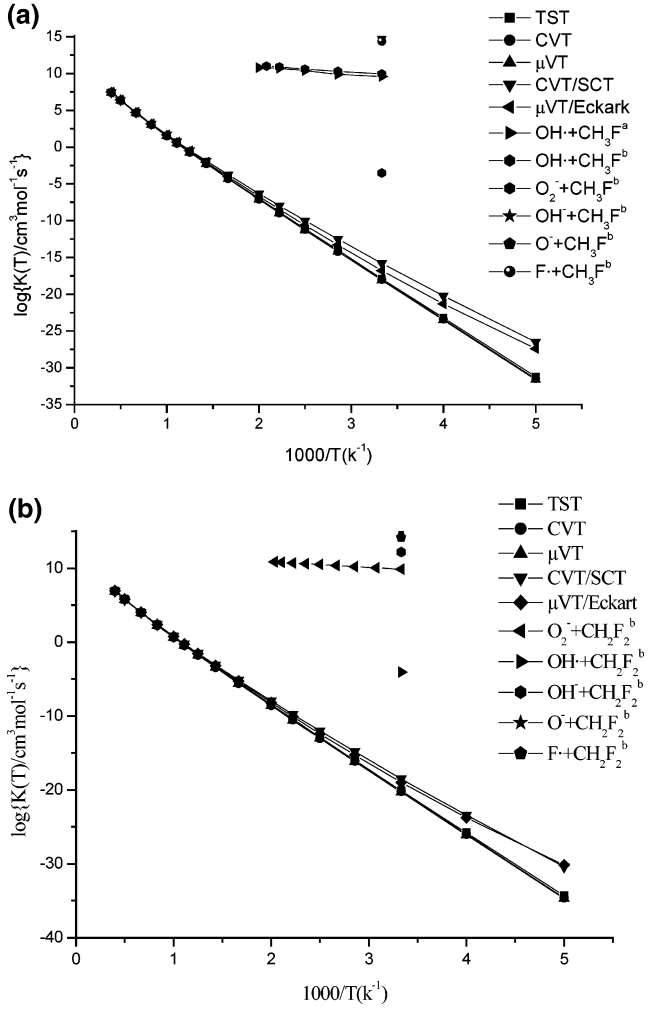

Figure 4. Calculated Arrhenius plots of the rate constants at the HL//MPW1K/6-31+G(d,p) level of theory of the reaction versus 1000/*T* (K^{-1}): (a) The reaction of ozone with fluoromethane. (b) The reaction of ozone with difluoromethane. [a]The TST/Eckart rate constant for the reaction of CH_3F with OH radical. [b]The experimental values from refs 15, 17, 21, 24, and 25.

3.3. Rate Constant Calculations. The TST, CVT, μVT, CVT/SCT, and μVT/Eckart rate constant calculations are carried out for a temperature range from 200 to 2500 K on the MPW1K/6-31+G(d,p) MEPs with energies refined at the HL//MPW1K/6-31+G(d,p) level of theory. The fitted three-parameter Arrhenius expressions of the calculated forward CVT/SCT and μVT/Eckart rate constants of the ozonolysis of fluoromethane are $k^{CVT/SCT}(T) = 2.76 \times 10^{-34}T^{5.81}e^{(-13975/T)}$ and $k^{\mu VT/Eckart}(T) = 1.15 \times 10^{-34}T^{5.97}e^{(-14530.7/T)}$, respectively. For the reaction of ozone with difluoromethane, the fitted three-parameter Arrhenius expressions of the calculated forward CVT/SCT and μVT/Eckart rate constants are $k^{CVT/SCT}(T) = 2.29 \times 10^{-36}T^{6.42}e^{(-15451.6/T)}$ and $k^{\mu VT/Eckart}(T) = 1.31 \times 10^{-36}T^{6.45}e^{(-15465.8/T)}$, respectively. Figure 4 shows the Arrhenius plots versus the temperatures.

The curves of TST, CVT, and μVT without tunneling correction nearly overlap in panels a and b of Figure 4 and indicate that the variational effect on the calculation of rate constants is small and can be ignored for the two reactions. For the reaction of ozone with fluoromethane, it could be found in Figure 4a that the curves CVT and the curves CVT/SCT are quite close at a temperature above 1000 K, and with the decrease of the temperature both curves become separate gradually. The

μVT/Eckart rate constants are consistently larger than the μVT rate constants. For example, the $k^{\mu VT/Eckart}/k^{\mu VT}$ factor of 1.11 at 2500 K and the corresponding factor increase to 166.01 at 250 K. These trends are quite obvious both in Figure 4a and b. The results tally with the character of the H-transfer reaction; the tunneling effect is crucial for the H-transfer reaction in the low-temperature area. For the reactions of both ozone with fluoromethane and ozone with difluoromethane, the CVT/SCT rate constants are slightly larger than the μVT/Eckart rate constants using HL//MPW1K method in the calculated temperature region. To validate the reliability of the HL method for the similar reaction system further, we also calculated the TST/Eckart rate constants of hydrogen abstraction reactions from CH_3F by OH radical (Figure 4). From Figure 4, one can find that the calculated rate constants are in good agreement with the available experimental values.[21]

The rate constants obtained by experiment technique for the reaction of $OH^•$, OH^-, O^-, O_2^-, $F^•$ with CH_3F and CH_2F_2 in the temperature range 300−500 K are also shown in Figure 4.[15,17,21,24,25] Because the values of the atmospheric lifetimes for fluoromethanes are needed to infer if the fluorinated hydrocarbons are really environmentally safe, it is worth comparing the reaction of $CH_nF_{4-n} + OH^•$, OH^-, O^-, O_2^-, $F^•$ with $CH_nF_{4-n} + O_3$ reactions. In the present study, the rate constant of the reaction of ozone with fluoromethane at 300−500 K is consistently smaller than the rate constants of the reaction of fluoromethane with other molecules, such as $OH^•$, OH^-, O^-, O_2^-, and $F^•$. Yet ozone concentration is many orders of magnitude larger than those of the radicals and anions, so the H-abstraction reactions by ozone may be very important in the low-temperature range. The rate constants increase rapidly with elevation of temperature. At 2500 K, the CVT/SCT and the μVT/Eckart rate constants of the reaction of O_3 with CH_3F are 4.50×10^{-17} and 4.87×10^{-17} cm^3 molecule^{-1} s^{-1}, respectively. At 2500 K, the CVT/SCT and the μVT/Eckart rate constants of the reaction of O_3 with CH_2F_2 are 8.72×10^{-17} and 9.24×10^{-17} cm^3 molecule^{-1} s^{-1}, respectively. Thus, the reactions should play a role under high-temperature conditions.

4. Summary

We present a theoretical study of reaction-path dynamics and rate constants of the bimolecular reaction of $CH_nF_{4-n} + O_3 \rightarrow HOOO + CH_{n-1}F_{4-n}$ ($n = 2,3$) over the wide temperature ranges. The bond lengths and bond angles for stable points obtained from different computational techniques are in good agreement with one another. The harmonic vibrational frequencies obtained from the MPW1K/6-31+G(d,p) level of theory agree with the available experimental data. The forward barrier heights of the ozonolysis of fluoromethane are smaller than those of ozonolysis of difluoromethane. With increasing number of fluorine substitution, the barrier height for the forward reaction increases. This reflects that the fluorine substitution can affect the H-abstraction process.

The extended Arrhenius expressions fitted from the CVT/SCT and μVT/Eckart rate constants of ozonolysis of fluoromethane in the temperature range 200−2500 K are $k^{CVT/SCT}(T) = 2.76 \times 10^{-34}T^{5.81}e^{(-13975/T)}$ and $k^{\mu VT/Eckart}(T) = 1.15 \times 10^{-34}T^{5.97}e^{(-14530.7/T)}$, respectively. For the reaction of ozone with difluoromethane, the fitted three-parameter Arrhenius expressions of the calculated forward CVT/SCT and μVT/Eckart rate constants are $k^{CVT/SCT}(T) = 2.29 \times 10^{-36}T^{6.42}e^{(-15451.6/T)}$ and $k^{\mu VT/Eckart}(T) = 1.31 \times 10^{-36}T^{6.45}e^{(-15465.8/T)}$, respectively. The calculated results show that the rate constants for two reactions have a positive temperature dependence in the temperature range 300−2500 K. Moreover, the variational effect is unimportant and the tunneling effect is not negligible in the low-temperature region for the title reactions.

According to the magnitude of the rate constants of the reactions for CH_3F and CH_2F_2 with $OH^•$, OH^-, O^-, O_2^-, $F^•$, and O_3 at about 300−500 K, we concluded that the rate constants of the reaction of ozone with fluoromethanes are consistently smaller than the rate constants of the reaction of fluoromethanes with $OH^•$, OH^-, O^-, O_2^-, and $F^•$ molecules. Yet ozone concentration is many orders of magnitude larger than those of the radicals and anions, so the H-abstraction reactions by ozone may be very important not only in low-temperature but also in the high-temperature conditions. It is anticipated that these kinetic data can be used to establish the modeling and testing methodologies that could be applied to larger molecules or to the complete reaction kinetic schemes for HFCs.

Acknowledgment. This work was supported by the National Natural Science Foundation of China (20373007) and the Excellent Young Teachers Program of MOE, People's Republic of China.

References and Notes

(1) Anderson, J. G.; Toohey, D. W.; Brune, W. H. *Science* **1991**, *251*, 39.
(2) McFarland, M. *Environ. Sci. Technol.* **1989**, *23*, 1203.
(3) Prather, M. J.; Wastson, R. T. *Nature* **1990**, *344*, 729.
(4) Rowland, F. S. *Ambio* **1990**, *19*, 281.
(5) Rowland, F. S. *Environ. Sci. Technol.* **1991**, *25*, 622.
(6) Smith, K. M.; Duxbury, G.; Newnham, D. A.; Ballard, J. *J. Chem. Soc., Faraday Trans.* **1997**, *93*, 2735.
(7) WMO Scientific Assessment of Ozone Depletion: 1989, World Meteorological Organization Global Ozone Research and Monitoring Project; WMO, 1990.
(8) *Montreal Protocol on Substances that Deplete the Ozone Layer*; United Nations Enviromental Programme, 1987.
(9) Hoffman, J. S. *Ambio* **1990**, *19*, 329.
(10) Berry, R. J.; Ehlers, C. J.; Burgess, D. R., Jr.; Zachariah, M. R.; Marshall, P. *Chem. Phys. Lett.* **1997**, *269*, 107.
(11) Zabarnick, S.; Fleming, J. W.; Lin, M. C. *Chem. Phys. Lett.* **1988**, *120*, 311.
(12) Rosenman, E.; McKee, M. L. *J. Am. Chem. Soc.* **1997**, *119*, 9033.
(13) Murray, C.; Retail, B.; Orr-Ewing, A. J. *Chem. Phys.* **2004**, *301*, 239.
(14) Hitsuda, K.; Takahashi, K.; Matsumi, Y. *J. Phys. Chem. A* **2001**, *105*, 5131.
(15) Peverall, R.; Kennedy, R. A.; Mayhew, C. A.; Watts, P. *Int. J. Mass Spectrom. Ion Processes* **1997**, *171*, 51.
(16) Yamamoto, M.; Yamashita, K.; Sadakata, M. *J. Mol. Struct. (THEOCHEM)* **2003**, *634*, 31.
(17) Bera, R. K.; Hanrahan, R. *Int. J. Radiat. Appl. Instrum., Part C* **1988**, *32*, 579.
(18) Gonzalez-Lafont, A.; Lluch, J. M.; Espinosa-Garcia, J. *J. Phys. Chem. A* **2001**, *105*, 10553.
(19) Bottonia, A.; Poggia, G.; Emmib, S. S. *J. Mol. Struct. (THEOCHEM)* **1993**, *279*, 299.
(20) Espinosa-Garcia, J.; Coitino, E. L.; Gonzalez-Lafont, A.; Lluch, J. M. *J. Phys. Chem. A* **1998**, *102*, 10715.
(21) Jeong, K.-M.; Kaufman, F. *J. Phys. Chem.* **1982**, *86*, 1808.
(22) Sun, L. P.; Song, K.; Hase, W. L.; Sena, M.; Riveros, J. M. *Int. J. Mass Spectrom.* **2003**, *227*, 315.
(23) Lee, E. P. F.; Dyke, J. M.; Mayhew, C. A. *J. Phys. Chem. A* **1998**, *102*, 8349.
(24) Mayhew, C. A.; Peverall, R.; Timperley, C. M.; Watts, P. *Int. J. Mass Spectrom.* **2004**, *233*, 155.
(25) Persky, A. *Chem. Phys. Lett.* **2003**, *376*, 181.
(26) Gritsenko, O. V.; Ensing, B.; Schipper, P. R. T.; Baerends, E. J. *J. Phys. Chem. A* **2000**, *104*, 8558.
(27) Tachikawa, H.; Igarashi, M. *Chem. Phys. Lett.* **1999**, *303*, 81.
(28) Cacace, F.; de Petris, G.; Pepi, F.; Troiani, A. *Science* **1999**, *285*, 81.
(29) Suma, K.; Sumiyoshi, Y.; Endo, Y. *Science* **2005**, *308*, 1885.
(30) Truhlar, D. G.; Garrett, B. C.; Klippenstein, S. J. *J. Phys. Chem.* **1996**, *100*, 12771.

(31) Truhlar, D. G.; Garrett, B. C. *Annu. Rev. Phys. Chem.* **1984**, *35*, 159.
(32) Truhlar, D. G.; Garrett, B. C. *J. Chem. Phys.* **1987**, *84*, 365.
(33) Truong, T. N. *J. Chem. Phys.* **1994**, *100*, 8014.
(34) Garrett, B. C.; Truhlar, D. G. *J. Phys. Chem.* **1979**, *83*, 1079.
(35) Hase, W. *Acc. Chem. Res.* **1998**, *31*, 659.
(36) Liu, Y.-P.; Lynch, G. C.; Truong, T. N.; Lu, D.-h.; Truhlar, D. G. *J. Am. Chem. Soc.* **1993**, *115*, 2408.
(37) Truhlar, D. G.; Isaacson, A. D.; Garrett, B. C. In *Theory of Chemical Reaction Dynamics*; Baer, M., Ed.; 1985; Vol. 4, p 65.
(38) Truhlar, D. G.; Isaacson, A. D.; Skodje, R. T.; Garrett, B. C. *J. Phys. Chem.* **1982**, *86*, 2252.
(39) Duncan, W. T.; Bell, R. L.; Troung, T. N. *J. Comput. Chem.* **1998**, *19*, 1039.
(40) Zhang, S.; Truong, T. N. *J. Phys. Chem. A* **2001**, *105*, 2427.
(41) Garrett, B. C.; Truhlar, D. G. *J. Phys. Chem.* **1979**, *83*, 2921.
(42) Lynch, B. J.; Fast, P. L.; Harris, M.; Truhlar, D. G. *J. Phys. Chem. A* **2000**, *104*, 4811.
(43) Lynch, B. J.; Truhlar, D. G. *J. Phys. Chem. A* **2003**, *107*, 3898.
(44) Becke, A. D. *J. Chem. Phys.* **1993**, *98*, 1372.
(45) Lee, C.; Yang, W.; Parr, R. G. *Phys. Rev. B* **1988**, *37*, 785.
(46) Becke, A. D. *J. Chem. Phys.* **1996**, *104*, 1040.
(47) Adamo, C.; Barone, V. *J. Chem. Phys.* **1998**, *108*, 664.
(48) Zhao, Y.; Truhlar, D. G. *J. Phys. Chem.* **2004**, *108*, 6908.
(49) Miller, J. A.; Klippenstein, S. J. *J. Phys. Chem. A* **2003**, *107*, 2680.
(50) Pople, J. A.; Head-Gordon, M.; Raghavachari, K. *J. Chem. Phys.* **1987**, *87*, 5968.
(51) Moller, C.; Plesst, M. S. *Phys. Rev.* **1934**, *46*, 618.
(52) Peterson, K. A.; Woon, D. E.; Dunning, T. H. *J. Chem. Phys.* **1994**, *100*, 7410.
(53) Woon, D. E.; Dunning, T. H. *J. Chem. Phys.* **1993**, *98*, 1358.
(54) Miller, J. A.; Klippenstein, S. J. *J. Phys. Chem. A* **2003**, *107*, 7783.
(55) Li, Q. S.; Zhang, X.; Zhang, S. W. *J. Phys. Chem. A* **2005**, *109*, 12027.
(56) Li, Q. S.; Luo, Q. *J. Phys. Chem. A* **2003**, *107*, 10435.
(57) Chase, M. W., Jr. *J. Phys. Chem. Ref. Data* **1998**, *9*, 1.
(58) Lias, S. G.; Karpas, Z.; Liebman, J. F. *J. Am. Chem. Soc.* **1985**, *107*, 6089.
(59) Frisch, M. J.; Trucks, G. W.; Schlegel, H. B.; Scuseria, G. E.; Robb, M. A.; Cheeseman, J. R.; Montgomery, J. A., Jr.; Vreven, T.; Kudin, K. N.; Burant, J. C.; Millam, J. M.; Iyengar, S. S.; Tomasi, J.; Barone, V.; Mennucci, B.; Cossi, M.; Scalmani, G.; Rega, N.; Petersson, G. A.; Nakatsuji, H.; Hada, M.; Ehara, M.; Toyota, K.; Fukuda, R.; Hasegawa, J.; Ishida, M.; Nakajima, T.; Honda, Y.; Kitao, O.; Nakai, H.; Klene, M.; Li, X.; Knox, J. E.; Hratchian, H. P.; Cross, J. B.; Adamo, C.; Jaramillo, J.; Gomperts, R.; Stratmann, R. E.; Yazyev, O.; Austin, A. J.; Cammi, R.; Pomelli, C.; Ochterski, J. W.; Ayala, P. Y.; Morokuma, K.; Voth, G. A.; Salvador, P.; Dannenberg, J. J.; Zakrzewski, V. G.; Dapprich, S.; Daniels, A. D.; Strain, M. C.; Farkas, O.; Malick, D. K.; Rabuck, A. D.; Raghavachari, K.; Foresman, J. B.; Ortiz, J. V.; Cui, Q.; Baboul, A. G.; Clifford, S.; Cioslowski, J.; Stefanov, B. B.; Liu, G.; Liashenko, A.; Piskorz, P.; Komaromi, I.; Martin, R. L.; Fox, D. J.; Keith, T.; Al-Laham, M. A.; Peng, C. Y.; Nanayakkara, A.; Challacombe, M.; Gill, P. M. W.; Johnson, B.; Chen, W.; Wong, M. W.; Gonzalez, C.; Pople, J. A. *Gaussian 03*; Gaussian, Inc.: Pittsburgh, PA, 2003.
(60) Werner, H. J.; Knowles, P. J.; et al. *MOLPRO 2002.1*; University of Birmingham: Birmingham, AL, 1999.
(61) Chuang, Y.-Y.; Corchado, J. C.; Fast, P. L.; Villa, J.; Hu, W.-P.; Liu, Y.-P.; Lynch, G. C.; Jackels, C. F.; Nguyen, K.; Gu, M. Z.; Rossi, I.; Coitino, E.; Clayton, S.; Melissas, V. S.; Lynch, B. J.; Steckler, R.; Garret, B. C.; Isaacson, A. D.; Truhlar, D. G. *POLYRATE*, 8.2 ed.; University of Minnesota: MN, 1999.
(62) Zhang, S.; Troung, T. N. VKLab; University of Utah, 2001.
(63) Kondo, S.; Nakanagi, T.; Sacki, S. *J. Chem. Phys.* **1980**, *73*, 5409.
(64) Kim, K.; King, W. T. *J. Chem. Phys.* **1980**, *73*, 5591.
(65) Jacox, M. E. *J. Phys. Chem. Ref. Data* **1984**, *13*, 945.
(66) Mizuno, M.; Saecki, S. *Spectrochim. Acta, Part A* **1976**, *32*, 1077.
(67) Barbe, A.; Secroun, C.; Jouve, P. *J. Mol. Struct.* **1974**, *49*, 171.